Preparation and characterization of H-shaped polylactide

Aristotelis Zografos, † Erin M. Maines, † Joseph F. Hassler, † Frank S. Bates, *, † Marc A. Hillmyer. *, ‡

[†]Department of Chemical Engineering and Materials Science, University of Minnesota, Minneapolis, MN, 55455-0132, United States

[‡] Department of Chemistry, University of Minnesota, Minneapolis, MN, 55455-0431, United States

*Corresponding authors (e-mail addresses: bates001@umn.edu; hillmyer@umn.edu)

Abstract

An H-polymer has an architecture that consists of four branches symmetrically attached to the ends of a polymer backbone, similar in shape to the letter 'H'. Here, a renewable H-polymer efficiently synthesized using only ring-opening transesterification is demonstrated for the first time. The strategy relies on a tetrafunctional poly(\pm -lactide) macroinitiator, from which four poly(\pm -lactide) branches are grown simultaneously. Proton nuclear magnetic resonance (1 H-NMR) spectroscopy, size exclusion chromatography (SEC), and matrix assisted laser desorption/ionization (MALDI) spectrometry were used to verify the macroinitiator purity. Branch growth was probed using 1 H-NMR spectroscopy and SEC to reveal unique transesterification phenomena that can be controlled to yield architecturally pure or more complex materials. H-shaped PLA was prepared at the multigram scale with a weight average molar mass $M_w > 100$ kg/mol and low dispersity D < 1.15. Purification involved routine precipitations steps, which yielded products that were architecturally relatively pure (\sim 93%). Small-amplitude oscillatory shear and extensional rheology measurements demonstrate the unique viscoelastic behavior associated with the H-shaped architecture.

TOC Image

Characterization:

¹H-NMR, MALDI, SEC, Rheology

With only two branch points, the H-polymer is one of the simplest non-linear macromolecular architectures. It consists of a central backbone with two arms that stem from each end, thus resembling the shape of the letter 'H'. H-polymers have been recognized for several decades as a basic platform for exploring how polymer architecture influences melt dynamics. This architecture contains a backbone segment that resists flow due to anchoring by the end segments, resulting in slow molecular relaxation. This resistance produces an advantageous property known as melt strain hardening, which improves polymer processability involving strong extensional flows encountered during techniques such as film blowing, foaming, and thermoforming. 1-4 Roovers and Toporowski reported the first successful synthesis of model H-shaped polymers using carbanionic polymerization.⁵ They coupled linear polystyrene chains together, resulting in a mixture of linear, star, and H-shaped homopolymers, subsequently purified through fractionation.⁵ Since then, limited progress towards new methods for synthesizing H-shaped homopolymers has been made. This is evidenced by several recent publications that still use the original polymers synthesized by Roovers et al. almost half a century ago. 6-8 To date, the only proven approach for synthesizing model H-shaped polymers based on a single polymerization technique still relies on carbanionic polymerization chemistry and all methods require polymer coupling.^{5, 9-15} The method enables independent molecular characterization of the polymer backbone and branches. However, the final coupling step tends to be inefficient at producing architecturally pure materials and requires rigorous fractionation procedures to isolate the desired H-polymers. Furthermore, the range of accessible monomers for carbanionic polymerization is limited (e.g., butadiene, isoprene, styrene). To improve the ease of large-scale synthesis and access to fully biobased H-shaped homopolymers – and subsequently biobased block polymers ¹⁶ – new approaches must be established.

Here, we report the first synthesis of H-shaped polylactide (PLA) made exclusively from ring-opening transesterification polymerization (ROTEP). We demonstrate the method can be accomplished at gram-scale while accessing high molar masses ($M_{\rm w} > 100$ kg/mol) and

maintaining a low dispersity of D < 1.15. We first synthesized a tetrafunctional PLA macroinitiator and subsequently grew branches from the ends to produce the H-polymer architecture. This approach avoids the use of chain coupling but does not readily allow independent molar mass characterization of the branches. Proton nuclear magnetic resonance (1 H-NMR) spectroscopy and matrix assisted laser desorption/ionization (MALDI) spectrometry were used to verify the purity of the macroinitiator. H-polymer growth was monitored in kinetic studies using size-exclusion chromatography (SEC) and 1 H-NMR spectroscopy. Based on this analysis, the resulting molecular architecture was ~ 93 wt% of the H version. Finally, small-amplitude oscillatory shear (SAOS) and extensional rheology were employed to characterize the distinct viscoelastic fingerprints associated with H-polymer melts.

H-shaped PLA was synthesized according to Scheme 1. First, the backbone was prepared by polymerizing ±-lactide from a dihydroxy initiator, yielding a linear chain with one hydroxy group at each chain-end (1, Scheme 1). The synthesis of polymers similar to 1 is well documented in the literature, ^{17, 18} and the associated ¹H-NMR characterization is shown in Figure S1. The number of hydroxy end groups was doubled by functionalizing 1 with the acetonide protected anhydride 2. The resulting protected macroinitiator 3 was then deprotected to yield the desired macroinitiator 4, which contains two hydroxy groups at each chain-end. Anhydride 2 was synthesized from 2,2-(hydroxymethyl)propionic acid (bis-MPA), which has found extensive use in dendrimer¹⁹⁻²⁵ and polymer synthesis²⁶⁻²⁸ over the last several decades. The synthesis of 2 is well documented in the literature and can be readily and efficiently carried out at gram-scale in only two steps.^{20, 22} The synthesis of 2 and the associated NMR characterization are described in the Supporting Information (Figures S2–S4). Using 4, H-shaped polylactide was synthesized by polymerizing ±-lactide from each of the hydroxy end-groups.

Scheme 1. Synthesis of H-shaped poly(\pm -lactide). A two-step and one-step approach were both demonstrated for the synthesis of **3**.

With a molar mass of $M_{\rm w}=8.2$ kg/mol (Figure S10), 3 can be synthesized in as little as 90 min and is purified simply through precipitation. Figure 1A shows the corresponding 1 H-NMR data of the purified polymer, which was made in two separate steps. The data suggests the end functionalization reaction was quantitative, which is evidenced by the complete replacement of the terminal lactide methine hydrogen at ~4.4 ppm (inset, polymer 1, Figure 1A) with a downfield signal at ~5.2 ppm due to deshielding of those protons upon functionalization. Quantitative conversion was confirmed by the integrations of the end-group chemical shifts (Figure 1A), which equate to their expected values when compared to the four aromatic hydrogens of the PLA midgroup.

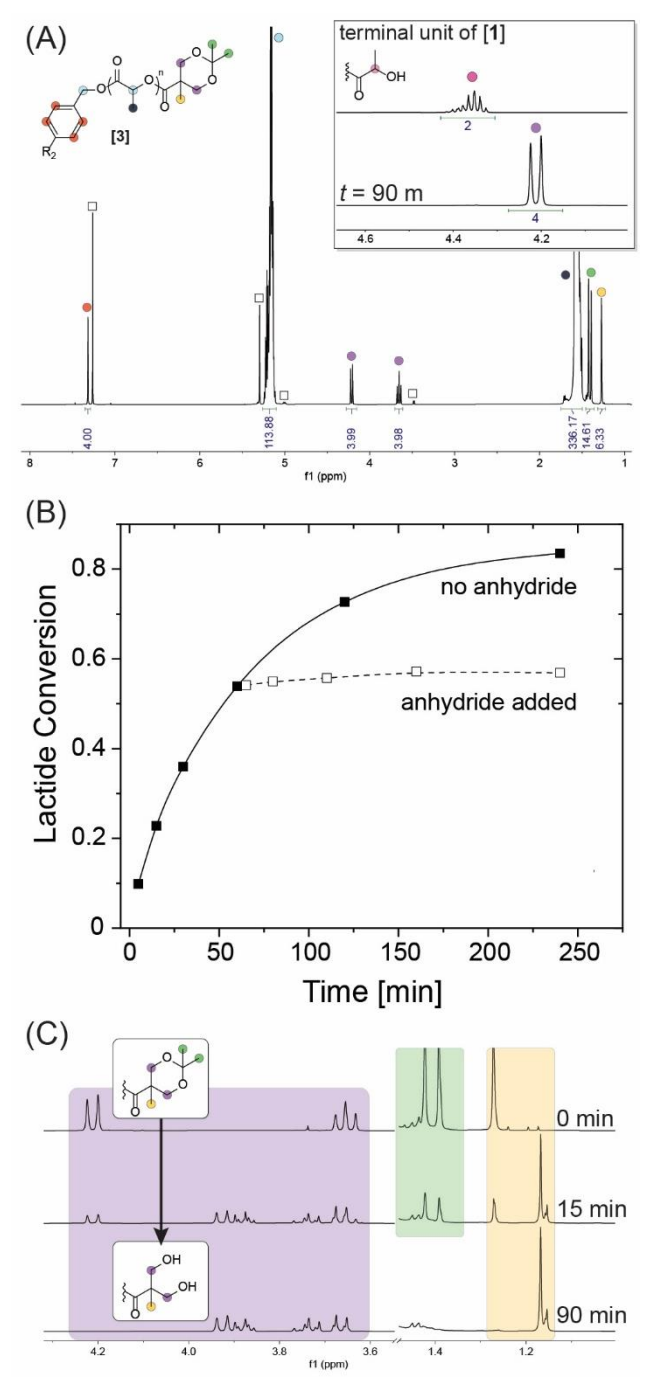


Figure 1. (A) ¹H-NMR data of **3** from the two-step synthesis in Scheme 1. The inset shows the terminal repeat unit **1**, highlighting the chemical shift at ~4.4 ppm that disappears as the reaction proceeds. Square symbols correspond to solvent residues (5.3 and 3.5 ppm) or residual monomer (5.0 ppm). (B) Lactide conversion plotted as a function of time showing how the addition of **2** terminates the polymerization. (C) ¹H-NMR kinetic analysis of the deprotection reaction that yields **4** in Scheme 1. The disappearance of the acetonide chemical shift at ~1.4 ppm is a clear marker of the reaction. Residual lactide (~1.4 ppm) and pentane (~1.2 ppm, 0 min) are also observed.

As shown in Scheme 1, a single pot reaction can also be used to yield 3 with similar results (Figure S5). Figure 1B shows kinetic data for this reaction. For the experiment, two polymerizations were run in parallel using equal reagent concentrations. At 60 min, a solution of anhydride 2 and DMAP was added to one of the flasks. Upon the addition of the anhydride, the lactide conversion stops under these conditions (Figures 1B, S6). Fast termination of all propagating chains is beneficial because it enables the molar mass distribution to remain narrow during the functionalization step. This strategy was used to synthesize a sample of polymer 3 with a low dispersity of D = 1.11 and higher molar mass of $M_w = 29.3$ kg/mol (Figure S11).

Figure 1C shows representative ¹H-NMR data of the deprotection reaction used to produce the tetrafunctional macroinitiator (4, Scheme 1). The data tracks the associated acid catalyzed hydrolysis as a function of time. Long reaction times would likely result in deleterious cleavage of the PLA ester groups, producing end-group impurities and an increase in the molar mass dispersity. Conversion can be tracked through the chemical shifts that are shown in Figure 1C. Notably, the acetonide CH₃ chemical shifts at 1.4 ppm vanish after 90 min for the 8.2 kg/mol version of polymer 3 (Figure 1C). A reaction time of 180 min was necessary for similar conversions for the larger macroinitiator of 29.3 kg/mol due to the lower end-group concentration. Given the center of chirality at the end of the polylactide chain, the multiplicity of the peaks between 3.6-4.2 ppm as the reaction progresses (purple region, Figure 1C) is evident. For reference, Figure S7 shows the end-group conversion as a function of time. For all macroinitiators synthesized, the end-group protons integrate to their expected value (Figures S8–S9) when referenced to the PLA mid-group. This provides further evidence for a quantitative reaction and indicates PLA hydrolysis did not occur to any significant extent. The absence of peaks at ~4.4 ppm (e.g., inset, Figure 1A) also indicates no PLA hydrolysis occurs, since the reaction would yield hydroxy end-groups. Additionally, SEC analysis of each macroinitiator shows that the molar mass remained narrow before and after the deprotection reactions, further evidence that the polylactide chains were not cleaved by water (Figure S10–S11).

MALDI was used to track the entire end-group functionalization process for the lower molar mass sample (Figure 2). All steps in the macroinitiator synthesis yield a unimodal and narrow molar mass distribution (Figure 2A) which is again consistent with the absence of significant PLA hydrolysis (i.e., $\bf 3$ to $\bf 4$ in Scheme 1). Considering all steps, each distribution shifts in an expected way based on the end-group modifications. In Figure 2B, discrete populations of N can be easily tracked based on the m/z value of each peak. This is determined using the equation,

$$N = \frac{m/z - m_{\text{Na}^{+}} - m_{\text{mid}} - 2m_{\text{end}}}{m_{\text{lactide}}},$$
 (1)

where $m_{\text{Na+}}$, m_{mid} , m_{end} , and m_{lactide} are the molar masses of the sodium counterion, polylactide midgroup, polylactide end-group, and lactide repeat unit, respectively. Substituting the expected values into Equation 1, based on the chemical structures in Scheme 1, yields integer values of $N \pm 0.02$ for each peak in the MALDI data. As an example, Figure 2B tracks the N = 50 population showing that it shifts within 0.3% of the expected m/z value as the end-group changes. Together, these observations strongly support quantitative yields of the anticipated end-groups.

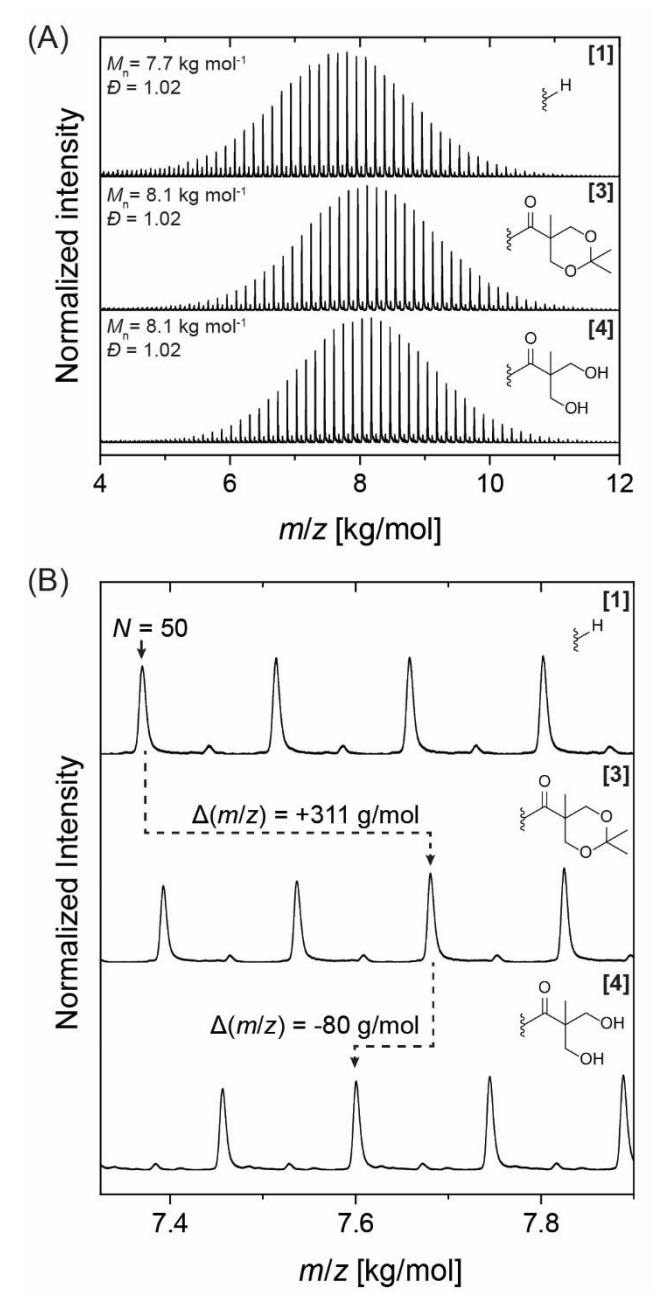


Figure 2. (A) MALDI data of 1, 3, and 4 from Scheme 1. The end-group structure is shown for each polymer. The number average molar mass and dispersity were both calculated from these data. (B) Expanded MALDI data, showing how the N = 50 population changes with the end-group modifications. The behavior is representative of all populations of N.

Growth of the H-polymer branches was monitored by ¹H-NMR spectroscopy and THF-SEC (Figures 3A,B). The ¹H-NMR data used in this analysis shows that the protons adjacent to the hydroxy end-groups completely shift downfield within 1 min (Figure S12). Importantly, this indicates that each end-group initiates a branch, since the chemical shifts of these protons are expected to change based on their new chemical environment upon initiation. Figure 3A shows the number average molar mass (M_n) and dispersity as a function of lactide conversion (see Equation S1). A linear increase in molar mass with conversion is evident, as expected for 1,8diazabicyclo(5.4.0)undec-7-ene (DBU) catalyzed polymerizations (Scheme 1).²⁹ At a conversion of ~80%, interchain transesterification rapidly increases the molar mass dispersity. 30, 31 In the synthesis of linear and star polymers grown from a discrete initiator, transesterification changes the molar mass distribution, but not the molecular architecture. However, this is not the case for the H-polymers described here. Transesterification can cleave the backbone, resulting in a mixture of branched species that becomes more complex over time, as illustrated in Figure 3A. This process does not change the total number of chains, which is why the number average molar mass (M_n) continues to scale linearly with monomer conversion in this region (Figure 3A). The presence of backbone transesterification can be clearly observed in the SEC elution profile for each time point. The different degrees of branching and molar masses of each population creates contrast in hydrodynamic volume, as suggested by the arrows shown in Figure 3B. This phenomenon is unique to polyesters containing more than one branch point under ROTEP conditions and is important to consider when synthesizing such materials.

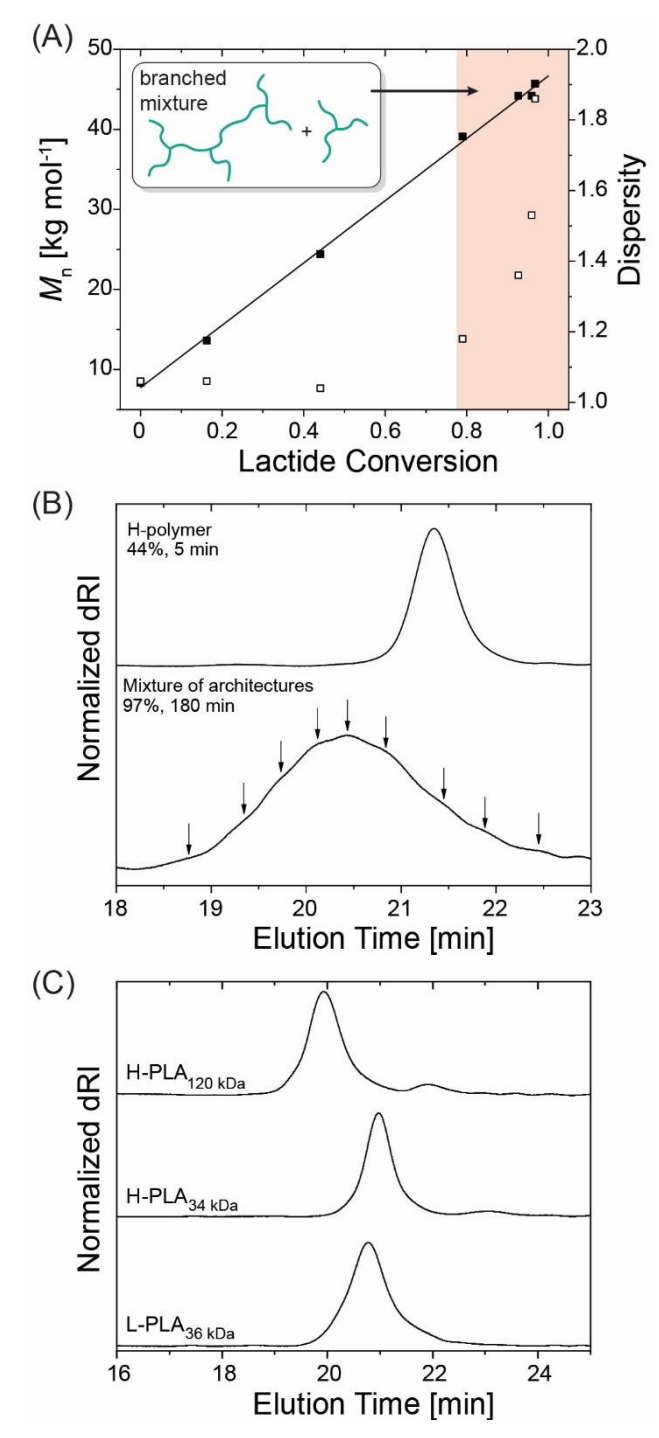


Figure 3. (A) H-polymer molar mass and dispersity as a function of lactide conversion. At high conversion, polymers with complex branching form due to transesterification. (B) Corresponding SEC elution profiles collected via differential refractometry. At high conversion, a multimodal distribution is obtained with each mode identified by an arrow. (C) SEC traces of the H-shaped and linear PLA used in the rheological analyses.

The molecular characterization detailed above demonstrates that H-shaped polymers were effectively synthesized according to Scheme 1. Successful H-polymer synthesis was further revealed through rheological measurements, comparing linear and H-shaped polylactide melts, designated as L-PLA_{xx} and H-PLA_{xx}; here the 'xx' subscript refers to the total weight average molar mass (M_w) in kg/mol. Details of the polymers that were synthesized at gram-scale are provided in Table 1, and Figure 3C shows the SEC elution profiles of each polymer. These H-polymers have a narrow dispersity $D_{RI} < 1.12$ and contain a small amount (~7 wt%) of impurity at longer elution times (i.e., smaller hydrodynamic volumes), possibly resulting from spurious water initiation during synthesis. The architecture of this impurity cannot be determined through the analysis presented here, though the molar mass is expected to be smaller. Low molar mass chains can speed up molecular relaxation through constraint release.^{7,32} However, at only 7 wt% we do not expect these impurities to have a substantial influence on the viscoelastic response.

Table 1. Molecular, thermal, and viscosity data for each polymer. The subscript 'bb' refers to the H-polymer backbone.

	$M_{\rm w}^{a}$ (kg mol ⁻¹)	\overline{D}^{b}	$M_{\rm w,bb}^{ c}$ (kg mol ⁻¹)	${\it extit{B}_{bb}}^{b,c}$	$M_{\rm w,arm}^{ d}$ (kg mol ⁻¹)	<i>T</i> _g (°C)	$\eta_0 \times 10^{-4f}$ (Pa·s)
L-PLA ₃₆	36	1.20				55.5	23.9
H-PLA ₃₄	34	1.09	8.2	1.13	6.2	50.0	5.00
H-PLA ₁₂₀	120	1.12	31.3	1.09	22.2	55.1	313

^aCalculated from SEC-MALS using a calculated dn/dc, which assumes 100% mass recovery.

^b Calculated from the differential refractometry data.

^c Determined from the SEC analyses (Figures S10-11) of the deprotected macroinitiators (4, Scheme 1)

^d Calculated using the equation $M_{\text{w,arm}} = (M_{\text{w}} - M_{\text{w,bb}})/4$.

^e Determined from differential scanning calorimetry data (Figure S13).

^fDetermined from the lowest measured frequency in the SAOS data (Figure S15).

Figure 4A shows master curves of each polymer collected using small amplitude oscillatory shear (SAOS) rheology. Comparisons of these results are made using a reference temperature of $T_{ref} = T_g + 34$ °C. The shift factors used in the analyses show no correlation to the polymer architecture when referenced to T_g (Figure S14), which is consistent with findings in the literature. This region corresponds to the Rouse dynamics of small chain sections not constrained by entanglements, where τ_e is the entanglement relaxation time. At this scale, the dynamics should be independent of the macromolecular architecture, in agreement with the overlapping data in this regime (Figure 1A, inset). This agreement indirectly supports the measured values of T_g from DSC (Figure S13) since each master curve was shifted with respect to those values (i.e., $T_{ref} = T_g + 34$ °C). For H-PLA₃₄, the T_g was found to be ~5 °C lower compared to the other materials (Table 1). We attribute this to the added number of end-groups, which improves chain mobility and decreases T_g based on free volume arguments. This effect diminishes with increasing molar mass of and, therefore, increasing the H-polymer molar mass to that of H-PLA₁₂₀ results in a T_g similar to L-PLA₃₆.

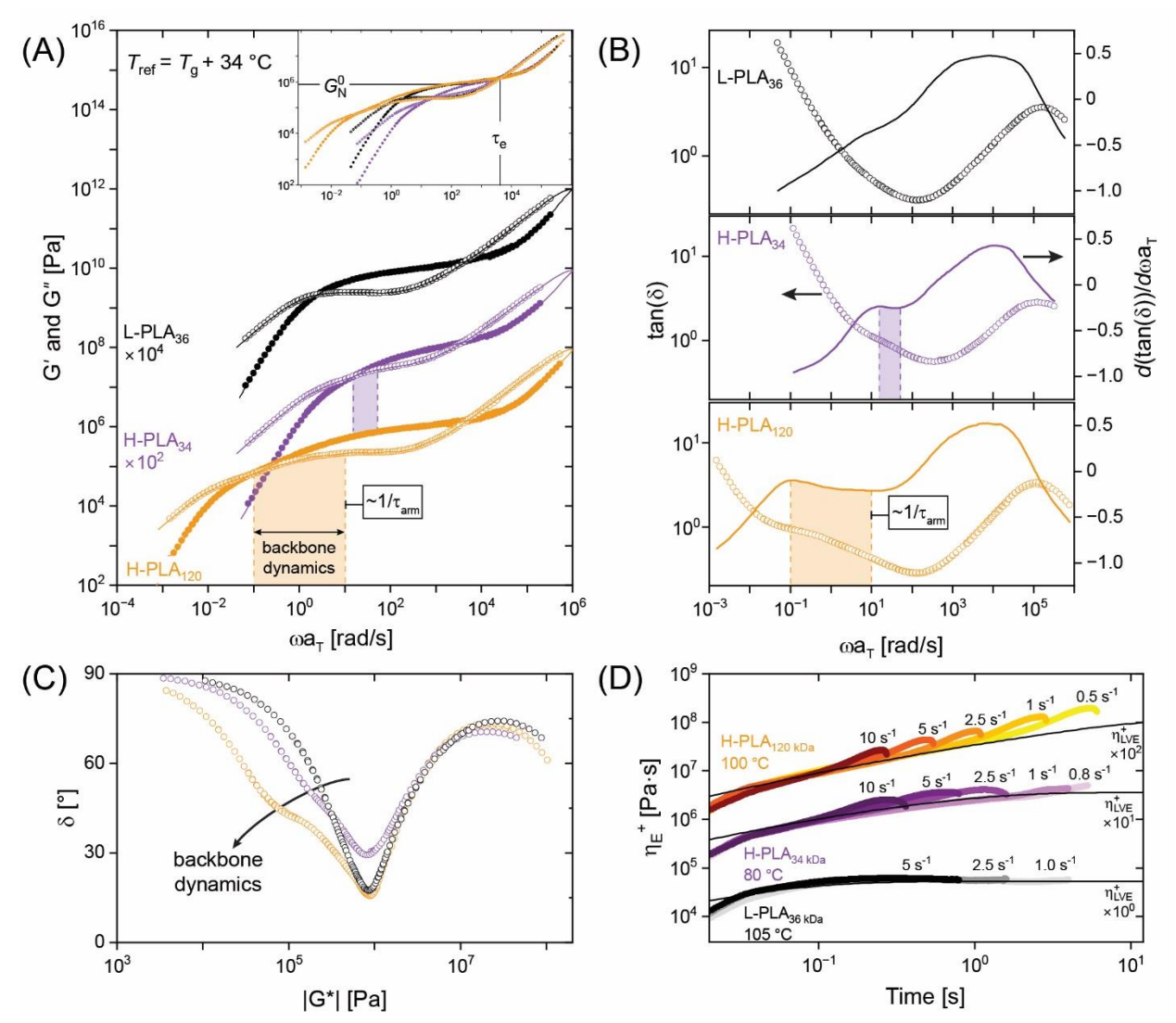


Figure 4. (A) Master curves of each polymer using a reference temperature $T_{\text{ref}} = T_{\text{g}} + 34$ °C. The data was fit to a multi-mode Maxwell model (Equation S3), indicated by the solid lines. The inset shows data without a vertical shift. (B) Tangent of the phase angle (δ) and its derivative plotted as a function of frequency. (C) Van Gurp-Palmen plots of each polymer melt. The 'kink' in the data indicated by the arrow is only observed for the H-polymers. (D) The transient extensional viscosity of each polymer melt measured at the indicated temperatures and plotted as a function of the deformation time. The solid lines correspond to the linear viscoelastic limits, calculated from Equation 3.

At ω < 1/ τ_e , each polymer shows a different dynamic response (Figure 4A). For L-PLA₃₆, a broad rubbery-like plateau is observed that stretches three orders of magnitude in frequency, characteristic of reptation dynamics. The associated entanglement molar mass was found to be $M_e = 3.6$ kg/mol using the equation

$$M_{\rm e} = \frac{4\rho RT_{\rm ref}}{5G_{\rm N}^0},^{32} \tag{2}$$

where R is the gas constant, G_N^0 is the plateau modulus determined from the minimum in the $\tan(\delta)$ curve, 32 and ρ is the melt density at the reference temperature $T_{\rm ref}$. The temperature dependence of ρ is reported by Witzki. 37 This value of $M_{\rm e}$ is consistent with values reported in the literature for polylactide. $^{38-40}$

Despite its similar molar mass, H-PLA₃₄ displays a notably different response than L-PLA₃₆ at $\omega < 1/\tau_e$. While the entanglement molar mass is virtually the same (i.e., $M_e = 3.8 \text{ kg/mol}$), the range in frequency of the plateau region is an order of magnitude smaller. Moving to frequencies below the plateau in G', a feature is observed for the H-polymer melts that is distinctly different compared to the linear L-PLA (highlighted regions, Figures 4A). The feature exists between two 'shoulders' in G'', more clearly seen in the first derivative of $tan(\delta)$, with respect to frequency (Figure 4B), where δ is the phase angle. In Figure 4C, δ is plotted versus the magnitude of the complex modulus ($|G^*|$), known as a van Gurp-Palmen plot. For each H-polymer melt, a 'kink' in the data is observed at low values of $|G^*|$, which is not found for the linear melt. Note, this feature is also absent in star polymer melts. 41, 42 Each of the unique phenomena in Figures 4A-C is due to the hierarchical relaxation mechanism that occurs in architectures with more than one branch point. This results in a backbone that is 'pinned' between branches that cannot diffuse until the multiple constraints created by the arms have been lifted (i.e., the arms have fully relaxed). This produces a frequency response in the dynamic moduli that is dominated by the backbone dynamics (Figure 4A, 4B), where the high frequency border likely approximates the inverse of the arm relaxation time $(1/\tau_{arm})$.

The zero-shear viscosity (η_0) of H-PLA₃₄ is roughly 5 times lower than that of L-PLA₃₆ (Table 1, Figure S15). η_0 is intrinsically related to the size of the polymer and its topological constraints (e.g., entanglements), hence it makes intuitive sense to normalize polymers by their size when comparing η_0 to better understand how topological constraints influence this property. Roovers *et al.* conducted such an analysis to compare H-polymer and linear polymer melts and

found the former to have a larger η_0 only when the number of arm entanglements was greater than $\sim 3.^{43}$ In this limit, the branches can form elastically effective constraints, which slows the dynamics exponentially with $M_{\rm w}$, resulting in a more viscous melt.^{32,43,44} Here, the branches of H-PLA₃₄ are not well entangled (i.e., $M_{\rm arm} < 3M_{\rm e}$, Table 1) and, as such, lower viscosity is expected.

Figure 4D plots the transient extensional viscosity ($\eta_{\rm E}^{+}$) as a function of time for each polymer. The linear viscoelastic envelope in extension ($\eta_{\rm E,\,LVE}^{+}$) was calculated using the following expression: ⁴⁵

$$\eta_{\text{E,LVE}}^+(t) \approx 3 \sum_{i=1}^N g_i \lambda_i (1 - \exp(-t/\lambda_i)).$$
(3)

The relaxation strengths (g_i) and time constants (λ_i) of each mode in equation 3 are provided in Tables S1-S3, and additional discussion of this modeling can be found in Section S5 of the Supporting Information. The temperatures probed were chosen based on the viscosity and stretch relaxation rates (τ_s) of each melt, which establishes the Hencky strain rates above which non-linear viscoelastic flow (e.g., melt strain hardening) can be explored. For the H-polymer melts, τ_s can be calculated using the approximate values of τ_{arm} shown in Figure 4A. More discussion regarding this analysis is provided in the Supporting Information (Section S5). The data shows clear evidence of melt strain hardening (MSH) for the H-PLA samples, which is absent in L-PLA₃₆. Due to the high viscosity of L-PLA₃₆, efforts to probe time-temperature regions associated with non-linear viscoelastic flow were unsuccessful. Attempts at lower temperatures or faster rates caused the sample to be pulled from the sample grips on the rheometer. Therefore, quantitative comparisons of non-linear viscoelasticity are not feasible between architectures. However, these observations underscore an important point: non-linear viscoelastic flow for H-polymers is more accessible, compared to linear chains of a similar molar mass. Therefore, these architectures are expected to facilitate processing, since MSH is advantageous for methods such as film blowing, thermoforming, and foaming. 1-4

An efficient strategy for synthesizing H-shaped polymers using ring-opening transesterification polymerization has been established. The successful synthesis was validated using a suite of molecular (i.e., ¹H-NMR spectroscopy, SEC, MALDI) and rheological (i.e., SAOS, extensional rheology) analyses. The method uses a telechelic macroinitiator, from which four arms can be polymerized to grow the H-polymer (Scheme 1). As the arms grow, we demonstrate that backbone transesterification can lead to a complex mixture of branched species at high monomer conversion. Thus, lower monomer conversion must be targeted to synthesize architecturally pure materials. Ostensibly, this can also be accomplished through judicious catalyst selection that limits transesterification. 17, 46, 47 We expect this strategy can be easily extended to other cyclic esters, such as caprolactone, valerolactone, and their derivatives, thus enabling access to a variety of Hshaped block polymers. 48 We demonstrate the H-shaped architecture to enable advantageous meltstrain hardening at lower strain rates compared to a linear polymer of similar molar mass. However, our initial results suggest that the branch molar mass only nominally influences the magnitude of this behavior.⁴⁹ Overall, these findings will improve experimental access to Hshaped polymers, enabling the community to probe theory and improve the melt processability of biobased plastics that underperform in strong extensional flows. The work readily lends itself towards the synthesis of block H-polyesters, which opens avenues for designing high-performance elastomers, tough thermoplastics, complex morphologies, and compatibilizers for recycling. 48, 50-52

Associated Content

The Supporting Information is available free of charge at:

Materials and methods, molecular characterization data and analysis, and rheology data and analysis.

Author Information

Corresponding Authors:

Marc A. Hillmyer – Department of Chemistry, University of Minnesota, Minneapolis, MN, 55455-0431, United States; orcid.org/0000-0001-8255-3853; Email: hillmyer@umn.edu

Frank S. Bates – Department of Chemical Engineering and Materials Science, University of Minnesota, Minneapolis, MN, 55455-0132, United States; orcid.org/0000-0003-3977-1278; Email: bates001@umn.edu

Authors:

Aristotelis Zografos – Department of Chemical Engineering and Materials Science, University of Minnesota, Minneapolis, MN, 55455-0132, United States; orcid.org/0000-0001-9612-091X

Erin M. Maines – Department of Chemical Engineering and Materials Science, University of Minnesota, Minneapolis, MN, 55455-0132, United States; orcid.org/0009-0002-8416-6333

Joseph F. Hassler – Department of Chemical Engineering and Materials Science, University of Minnesota, Minneapolis, MN, 55455-0132, United States; orcid.org/0000-0003-0904-2314

Notes

The authors declare no competing financial interests.

The data from this study are openly available in the Data Repository for University of Minnesota (DRUM) at (insert hyperlink to DRUM database, which will be done pending publication).

Acknowledgements

Support for this work was provided by the National Science Foundation (NSF) Center for Sustainable Polymers (CHE-1901635) at the University of Minnesota, as well as the NSF Graduate Research Fellowship Program (DGE-1839286). We would like to thank the Minnesota NMR Center for providing access to their instruments. Some of the NMR experiments were conducted using an instrument that is supported by the Director, National Institutes of Health (S10OD011952). The content of this work is solely the responsibility of the authors and does not necessarily represent the official views of the National Institutes of Health. We would like to thank Prof. Thomas R. Hoye and Dr. Benjamin R. Reiner for helpful discussions related to the NMR

analyses. We would like to thank Kate Wortman-Otto for providing the linear polylactide sample (L-PLA₃₆). We also thank Todd Markowski for assistance with the MALDI spectrometry data collection, as well as Emily Ness for assistance with SEC data collection. The authors also thank Mahesh Mahanthappa for his helpful synthesis advice, especially with regards to the deprotection reaction. The viscoelastic data was analyzed with the help of IRIS Rheohub; we thank Prof. H. Henning Winter for providing access to this software. Lastly, we would like to thank Dr. Yoon-Jung Jang, Daniel Krajovic, and Prof. Caitlin Sample for helpful discussions related to the research.

References

- (1) Münstedt, H. Extensional Rheology and Processing of Polymeric Materials. **2018**, *33* (5), 594-618.
- (2) Münstedt, H.; Kurzbeck, S.; Stange, J. Importance of elongational properties of polymer melts for film blowing and thermoforming. *Polymer Engineering & Science* **2006**, *46* (9), 1190-1195.
- (3) Münstedt, H.; Steffl, T.; Malmberg, A. Correlation between rheological behaviour in uniaxial elongation and film blowing properties of various polyethylenes. *Rheologica Acta* **2005**, *45* (1), 14-22.
- (4) Spitael, P.; Macosko, C. W. Strain hardening in polypropylenes and its role in extrusion foaming. *Polymer Engineering & Science* **2004**, *44* (11), 2090-2100.
- (5) Roovers, J.; Toporowski, P. M. Preparation and characterization of H-shaped polystyrene. *Macromolecules* **1981**, *14* (5), 1174-1178.
- (6) Ianniello, V.; Costanzo, S. Linear and nonlinear shear rheology of nearly unentangled H-polymer melts and solutions. *Rheologica Acta* **2022**, *61* (10), 667-679.
- (7) Lentzakis, H.; Costanzo, S.; Vlassopoulos, D.; Colby, R. H.; Read, D. J.; Lee, H.; Chang, T.; van Ruymbeke, E. Constraint Release Mechanisms for H-Polymers Moving in Linear Matrices of Varying Molar Masses. *Macromolecules* **2019**, *52* (8), 3010-3028.
- (8) Snijkers, F.; Lee, H.; Chang, T.; Das, C.; Vlassopoulos, D. Start-up shear flow of a well-characterized entangled H-polymer. *European Polymer Journal* **2024**, *206*, 112806.
- (9) Chen, X.; Rahman, M. S.; Lee, H.; Mays, J.; Chang, T.; Larson, R. Combined Synthesis, TGIC Characterization, and Rheological Measurement and Prediction of Symmetric H Polybutadienes and Their Blends with Linear and Star-Shaped Polybutadienes. *Macromolecules* **2011**, *44* (19), 7799-7809.
- (10) Rahman, M. S.; Aggarwal, R.; Larson, R. G.; Dealy, J. M.; Mays, J. Synthesis and Dilute Solution Properties of Well-Defined H-Shaped Polybutadienes. *Macromolecules* **2008**, *41* (21), 8225-8230
- (11) Rahman, M. S.; Lee, H.; Chen, X.; Chang, T.; Larson, R.; Mays, J. Model Branched Polymers: Synthesis and Characterization of Asymmetric H-Shaped Polybutadienes. *ACS Macro Letters* **2012**, *1* (5), 537-540.
- (12) Perny, S.; Allgaier, J.; Cho, D.; Lee, W.; Chang, T. Synthesis and Structural Analysis of an H-Shaped Polybutadiene. *Macromolecules* **2001**, *34* (16), 5408-5415.
- (13) Hakiki, A.; Young, R. N.; McLeish, T. C. B. Synthesis and Characterization of H-Shaped Polyisoprene. *Macromolecules* **1996**, *29* (10), 3639-3641. (14) Hadjichristidis, N.; Xenidou, M.; Iatrou, H.; Pitsikalis, M.; Poulos, Y.; Avgeropoulos, A.;
- (14) Hadjichristidis, N.; Xenidou, M.; Iatrou, H.; Pitsikalis, M.; Poulos, Y.; Avgeropoulos, A.; Sioula, S.; Paraskeva, S.; Velis, G.; Lohse, D. J.; et al. Well-Defined, Model Long Chain Branched Polyethylene. 1. Synthesis and Characterization. *Macromolecules* **2000**, *33* (7), 2424-2436.

- (15) Takahata, K.; Uchida, S.; Goseki, R.; Ishizone, T. Synthesis of chain end acyl-functionalized polymers by living anionic polymerization: versatile precursors for H-shaped polymers. *Polymer Chemistry* **2019**, *10* (29), 3951-3959.
- (16) Meier-Merziger, M.; Imschweiler, J.; Hartmann, F.; Niebuur, B.-J.; Kraus, T.; Gallei, M.; Frey, H. Bifunctional Carbanionic Synthesis of Fully Bio-Based Triblock Structures Derived from β-Farnesene and Il-Dilactide: Thermoplastic Elastomers. *Angewandte Chemie International Edition* **2023**, *62* (42), e202310519.
- (17) Dove, A. P. Organic Catalysis for Ring-Opening Polymerization. *ACS Macro Letters* **2012**, *1* (12), 1409-1412.
- (18) Kiesewetter, M. K.; Shin, E. J.; Hedrick, J. L.; Waymouth, R. M. Organocatalysis: Opportunities and Challenges for Polymer Synthesis. *Macromolecules* **2010**, *43* (5), 2093-2107.
- (19) García-Gallego, S.; Nyström, A. M.; Malkoch, M. Chemistry of multifunctional polymers based on bis-MPA and their cutting-edge applications. *Progress in Polymer Science* **2015**, *48*, 85-110
- (20) Ihre, H.; Hult, A.; Fréchet, J. M. J.; Gitsov, I. Double-Stage Convergent Approach for the Synthesis of Functionalized Dendritic Aliphatic Polyesters Based on 2,2-Bis(hydroxymethyl)propionic Acid. *Macromolecules* **1998**, *31* (13), 4061-4068.
- (21) Ihre, H.; Padilla De Jesús, O. L.; Fréchet, J. M. J. Fast and Convenient Divergent Synthesis of Aliphatic Ester Dendrimers by Anhydride Coupling. *Journal of the American Chemical Society* **2001**, *123* (25), 5908-5917.
- (22) Malkoch, M.; Malmström, E.; Hult, A. Rapid and Efficient Synthesis of Aliphatic Ester Dendrons and Dendrimers. *Macromolecules* **2002**, *35* (22), 8307-8314.
- (23) Montañez, M. I.; Campos, L. M.; Antoni, P.; Hed, Y.; Walter, M. V.; Krull, B. T.; Khan, A.; Hult, A.; Hawker, C. J.; Malkoch, M. Accelerated Growth of Dendrimers via Thiol–Ene and Esterification Reactions. *Macromolecules* **2010**, *43* (14), 6004-6013.
- (24) García-Gallego, S.; Andrén, O. C. J.; Malkoch, M. Accelerated Chemoselective Reactions to Sequence-Controlled Heterolayered Dendrimers. *Journal of the American Chemical Society* **2020**, *142* (3), 1501-1509.
- (25) Östmark, E.; Macakova, L.; Auletta, T.; Malkoch, M.; Malmström, E.; Blomberg, E. Dendritic Structures Based on Bis(hydroxymethyl)propionic Acid as Platforms for Surface Reactions. *Langmuir* **2005**, *21* (10), 4512-4519.
- (26) Pitet, L. M.; Chamberlain, B. M.; Hauser, A. W.; Hillmyer, M. A. Synthesis of Linear, H-Shaped, and Arachnearm Block Copolymers By Tandem Ring-Opening Polymerizations. *Macromolecules* **2010**, *43* (19), 8018-8025.
- (27) Jikei, M.; Suzuki, M.; Itoh, K.; Matsumoto, K.; Saito, Y.; Kawaguchi, S. Synthesis of Hyperbranched Poly(l-lactide)s by Self-Polycondensation of AB2 Macromonomers and Their Structural Characterization by Light Scattering Measurements. *Macromolecules* **2012**, *45* (20), 8237-8244.
- (28) Fischer, A. M.; Wolf, F. K.; Frey, H. Long-Chain Branched Poly(Lactide)s Based on Polycondensation of AB2-type Macromonomers. *Macromolecular Chemistry and Physics* **2012**, 213 (13), 1349-1358.
- (29) Kamber, N. E.; Jeong, W.; Waymouth, R. M.; Pratt, R. C.; Lohmeijer, B. G. G.; Hedrick, J. L. Organocatalytic Ring-Opening Polymerization. *Chemical Reviews* **2007**, *107* (12), 5813-5840.
- (30) Watts, A.; Kurokawa, N.; Hillmyer, M. A. Strong, Resilient, and Sustainable Aliphatic Polyester Thermoplastic Elastomers. *Biomacromolecules* **2017**, *18* (6), 1845-1854.
- (31) Martello, M. T.; Burns, A.; Hillmyer, M. Bulk Ring-Opening Transesterification Polymerization of the Renewable δ -Decalactone Using an Organocatalyst. *ACS Macro Letters* **2012**, I(1), 131-135.
- (32) Dealy, J. M.; Read, D. J.; Larson, R. G. Structure and Rheology of Molten Polymers; Hanser, 2018. DOI: https://doi.org/10.3139/9781569906125.fm.
- (33) Kapnistos, M.; Lang, M.; Vlassopoulos, D.; Pyckhout-Hintzen, W.; Richter, D.; Cho, D.; Chang, T.; Rubinstein, M. Unexpected power-law stress relaxation of entangled ring polymers. *Nature Materials* **2008**, *7* (12), 997-1002.

- (34) Roovers, J. E. L.; Toporowski, P. M. The glass transition temperature of star-shaped polystyrenes. *Journal of Applied Polymer Science* **1974**, *18* (6), 1685-1691.
- (35) Wooley, K. L.; Hawker, C. J.; Pochan, J. M.; Frechet, J. M. J. Physical properties of dendritic macromolecules: a study of glass transition temperature. *Macromolecules* **1993**, *26* (7), 1514-1519.
- (36) Lodge, T. P.; Hiemenz, P. C. Polymer Chemistry; CRC Press, 2007.
- (37) Witzke, D. R. Introduction to properties, engineering, and prospects of polylactide polymers. Michigan State University, 1997.
- (38) Dorgan, J. R.; Janzen, J.; Clayton, M. P.; Hait, S. B.; Knauss, D. M. Melt rheology of variable L-content poly(lactic acid). *Journal of Rheology* **2005**, *49* (3), 607-619.
- (39) Martinetti, L. Uniaxial Extensional Behavior of A–B–A Thermoplastic Elastomers: Structure-Properties Relationship and Modeling. University of Minnesota, 2015. (accessed 08-09-2023).
- (40) Randall, J.; Flodquist, M.; Schroeder, J.; Valentine, J. R.; Owusu, O.; McCarthy, K.; Weed, J.; Hennen, J.; Heuzey, M. C.; Carreau, P. J. Comparing the Structural, Thermal, and Rheological Properties of Poly(meso-lactide) to Poly(l-lactide) and Poly(rac-lactide). *Macromolecules* **2024**.
- (41) Zografos, A.; All, H. A.; Chang, A. B.; Hillmyer, M. A.; Bates, F. S. Star-to-Bottlebrush Transition in Extensional and Shear Deformation of Unentangled Polymer Melts. *Macromolecules* **2023**, *56* (6), 2406-2417.
- (42) Wagner, M. H.; Narimissa, E.; Huang, Q. Analysis of elongational flow of star polymers. *Rheologica Acta* **2022**, *61* (6), 415-425.
- (43) Roovers, J. Melt rheology of H-shaped polystyrenes. *Macromolecules* **1984**, *17* (6), 1196-1200.
- (44) Rubinstein, M.; Colby, R. H. *Polymer Physics*; Oxford University Press, 2003.
- (45) López-Barrón, C. R.; Shivokhin, M. E.; Hagadorn, J. R. Extensional rheology of highly-entangled α-olefin molecular bottlebrushes. *Journal of Rheology* **2019**, *63* (6), 917-926.
- (46) Dove, A. P.; Pratt, R. C.; Lohmeijer, B. G. G.; Waymouth, R. M.; Hedrick, J. L. Thiourea-Based Bifunctional Organocatalysis: Supramolecular Recognition for Living Polymerization. *Journal of the American Chemical Society* **2005**, *127* (40), 13798-13799.
- (47) Pratt, R. C.; Lohmeijer, B. G. G.; Long, D. A.; Lundberg, P. N. P.; Dove, A. P.; Li, H.; Wade, C. G.; Waymouth, R. M.; Hedrick, J. L. Exploration, Optimization, and Application of Supramolecular Thiourea—Amine Catalysts for the Synthesis of Lactide (Co)polymers. *Macromolecules* **2006**, *39* (23), 7863-7871.
- (48) Park, S. J.; Bates, F. S.; Dorfman, K. D. Single gyroid in H-shaped block copolymers. *Physical Review Materials* **2023**, *7* (10), 105601.
- (49) Ianniruberto, G.; Marrucci, G. Entangled Melts of Branched PS Behave Like Linear PS in the Steady State of Fast Elongational Flows. *Macromolecules* **2013**, *46* (1), 267-275.
- (50) Bates, C. M.; Bates, F. S. 50th Anniversary Perspective: Block Polymers—Pure Potential. *Macromolecules* **2017**, *50* (1), 3-22.
- (51) Ruzette, A.-V.; Leibler, L. Block copolymers in tomorrow's plastics. *Nature Materials* **2005**, 4 (1), 19-31.
- (52) Self, J. L.; Zervoudakis, A. J.; Peng, X.; Lenart, W. R.; Macosko, C. W.; Ellison, C. J. Linear, Graft, and Beyond: Multiblock Copolymers as Next-Generation Compatibilizers. *JACS Au* **2022**, *2* (2), 310-321.